J. Geomag. Geoelectr., 47, 1197–1213, 1995

Initial Results from the 210° Magnetic Meridian Project—Review

Kiyohumi YUMOTO[1] and THE 210° MM MAGNETIC OBSERVATION GROUP

[1]*Solar-Terrestrial Environment Laboratory, Nagoya University, 3-13 Honohara, Toyokawa, Aichi 442, Japan*

(Received December 13, 1994; Revised September 4, 1995; Accepted September 12, 1995)

In order to understand the global magnetospheric responses to solar wind changes and to investigate the transfer (or propagation) processes and latitudinal structures of magnetospheric disturbances, coordinated ground-based observations along the 210° magnetic meridian (MM) are being conducted by the Solar-Terrestriai Environment Laboratory, Nagoya University in cooperation with 27 organizations in Australia, Indonesia, Japan, Papua New Guinea, the Philippines, Russia, Taiwan, and the United States (Yumoto *et al.*, 1992). In this paper, we review the initial results obtained from the 210° MM project; (1) a northern and southern hemisphere asymmetry for sudden commencements (sc) and sudden impulses (si), (2) low-latitude aurorae, (3) cavity-like and field line Pc 3-4 resonances stimulated by sc and si, (4) peculiarities of Pc 3 at low latitudes, and (5) the latitudinal profile of Pi 2.

1. Northern and Southern Hemisphere Asymmetry of sc and si

Sudden commencements (sc) are global magnetospheric phenomena caused by interplanetary shocks and other discontinuities. When the interplanetary magnetic field turns southward or becomes turbulent behind an interplanetary shock or discontinuity, geomagnetic storms can develop following so-called storm sudden commencements (ssc). When the interplanetary magnetic field remains northward behind the shocks or discontinuities, sc are not followed by geomagnetic storms. Although such sc have been called si (sudden impulses), there is no difference between the physical mechanisms producing ssc and si. Ground studies of sc made great progress after the International Geophysical Year (1957–1958). As described in a review by Araki (1994), the electric currents responsible for sc flow over a range of locations from the magnetopause to the inside of the Earth. The sc can be used to study the transient responses of the magnetosphere, ionosphere, and conducting Earth system to solar wind dynamic pressure variations.

The disturbance fields of sc and si observed on the ground can be subdivided into two subfields, DL and DP (Araki, 1994). The DL field is produced by electric currents flowing on the magnetopause and a propagating compressional wave front in the magnetosphere. DP fields are produced by twin vortex-type ionospheric currents, which are caused by a dawn-to-dusk electric field transmitted to the polar ionosphere. In order to examine which components of the DL and DP fields dominate sc and si magnetic variations on the ground, i.e., to investigate transfer processes and latitudinal structures of sc and si disturbances from the magnetopause through the magnetosphere to the Earth's surface and/or from the magnetopause to the polar ionosphere and thence to the magnetic equator, we analyzed magnetic field data from the 210° magnetic meridian (MM) chain of stations. Yumoto *et al.* (1992) provide full details concerning the 210° MM magnetic observations and instrumentations.

Figure 1 shows the H components of ordinary magnetograms during the course of a geomagnetic storm at the following 210° MM chain stations: Tixie (L = 5.89), Chokurdakh (5.46), Magadan (2.83), Paratunka (2.10), Moshiri (1.59), Onagawa (1.38), Kagoshima (1.22), Chichijima (1.14), and Guam (1.01) in the northern hemisphere and Biak (1.05), Darwin (1.18), Weipa (1.18), Learmonth (1.46), Birdsville (1.55), Dalby (1.57), Adelaide (2.11), and Macquarie Island (5.40) in the southern hemisphere. Table 1 summarizes station names, geographic and geomagnetic coordinates, and L values of the stations. The geomagnetic storm began with an sc ($\Delta H \sim 44.1$ nT at Birdsville) at 0615 UT on December 17, 1992. It is noteworthy that the amplitudes of sc and long-period (around 1 h) variations in the initial phase of

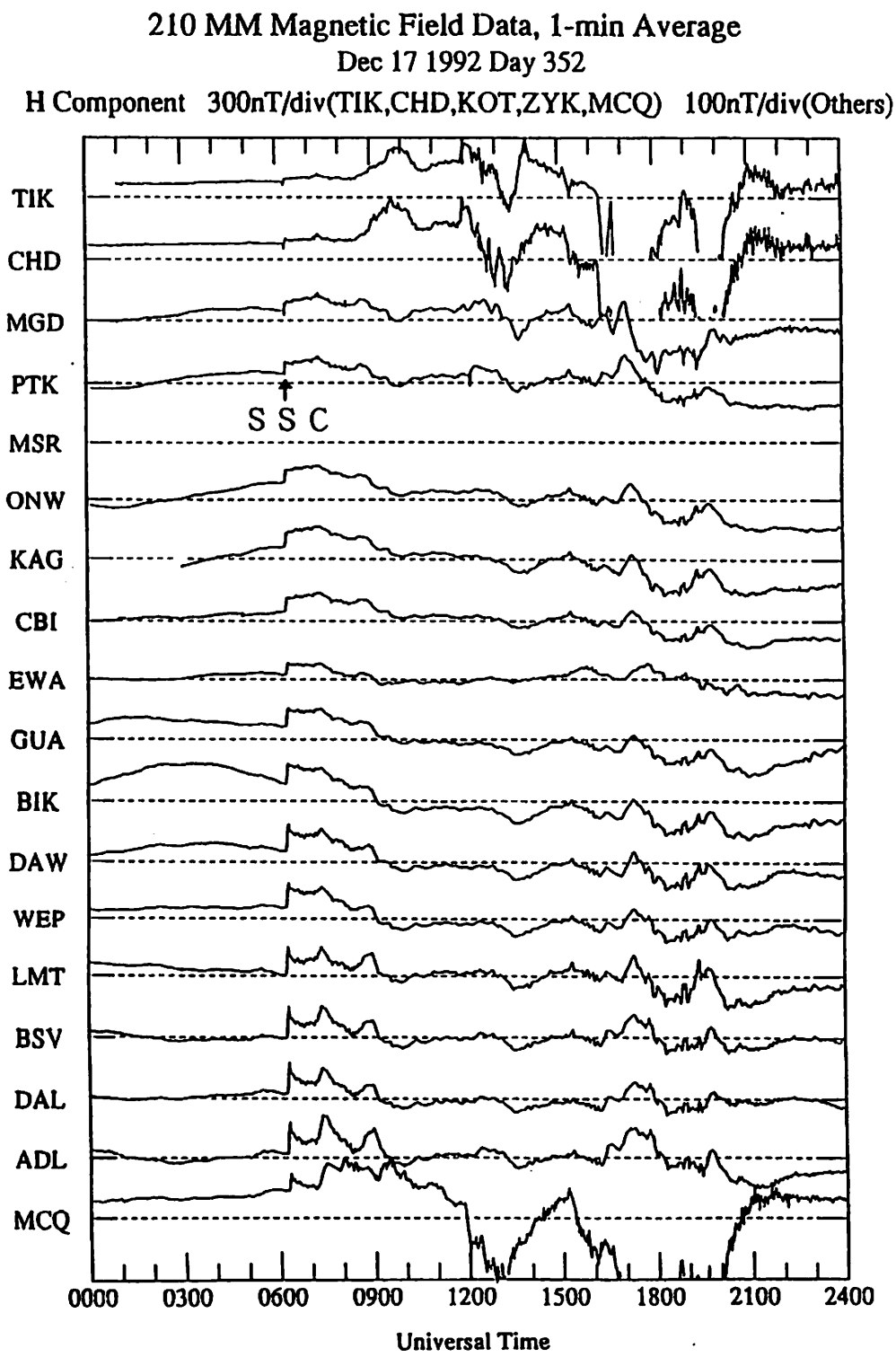

Fig. 1. Amplitude-time records of *H*-component ordinary magnetic variations during sc magnetic storm observed on December 17, 1992, at the 210° MM chain stations of TIK, CHD, MGD, PTK, MSR, ONW, KAG, CBI, EWA, and GUA in the northern hemisphere and BIK, DAW, WEP, LMT, BSV, DAL, ADL, and MCQ in the southern hemisphere (see Table 1).

a magnetic storm are larger in the southern (i.e., summer) hemisphere than in the northern (winter) hemisphere. We statistically analyzed 41 events of sc and si magnetic variations observed along the 210° meridian during the 15 months from November 1992 through January 1994 and found that the amplitudes of sc and si at low and middle latitudes are larger in the summer hemisphere than in the winter hemisphere.

Table 1. Station names, geographic and geomagnetic coordinates, and L values of proposed observation sites.

Station name*	Abbreviation	Geographic coordinates		Geomagnetic coordinates**		L**	Associ. inst.***	Date of onset
		Lat., deg	Long., deg	Lat., deg	Long., deg			
Tixie	TIK	71.59	128.78	65.67	196.88	5.89	IKFIA, IFZ	92/8–
Zhigansk	ZGN	66.75	123.26	61.01	193.82	4.25	IKFIA	
Yakutsk	YAK	62.02	129.72	56.08	200.51	3.21	IKFIA	
Irkutsk	IRT	52.17	104.45	47.13	177.01	2.16	ISTP	
Beijing	BJI	40.06	116.18	34.37	188.40	1.47	IGCAS	
Lunping	LNP	25.00	121.17	13.80	189.50	1.06	NCU, LNP	94/1–
Muntinlupa	MUT	14.37	121.02	3.58	191.57	1.00	CGSD	93/7–
Pontianak	PTN	–0.05	109.25	–11.37	180.49	1.04	LAPAN	
Watukosek	WTK	–7.56	112.63	–18.52	183.85	1.11	LAPAN	
Learmonth	LMT	–22.22	114.10	–34.15	185.02	1.46	IPS, UNC	91/8–
Katanning	KAT	–33.68	117.62	–46.63	188.24	2.12	GSARI, UNC	95/8–
Kotel'nyy	KTN	75.94	137.71	69.94	201.02	8.50	IKFIA	94/10–
Chokurdakh	CHD	70.62	147.89	64.67	212.12	5.46	IKFIA, IFZ	92/8–
Zyryanka	ZYK	65.75	150.78	59.62	216.72	3.91	IKFIA	94/4–
Magadan	MGD	59.97	150.86	53.56	218.66	2.83	IKIR	92/8–
St. Paratunka	PTK	52.94	158.25	46.34	225.91	2.10	IKIR	92/8–
Moshiri	MSR	44.37	142.27	37.61	213.23	1.59	STEL	90/7–
Onagawa	ONW	38.43	141.47	31.65	212.51	1.38	THU	91/6–
Kagoshima	KAG	31.48	130.72	25.13	202.24	1.22	STEL	90/7–
Chichijima	CBI	27.15	142.30	20.59	213.00	1.14	KMO	90/7–
Guam	GUA	13.58	144.87	4.57	214.76	1.01	USGS	91/6–
Yap	YAP	9.3	138.5	–0.3	209.0	1.00	UK	93/1–
Koror	KOR	7.33	134.50	–2.64	205.21	1.00	UAF	94/8–
Biak	BIK	–1.08	136.05	–12.18	207.30	1.05	LAPAN	92/5–
Wewak	WEW	–3.55	143.62	–14.14	215.27	1.06	PWH, UPNG	91/6–
Darwin	DAW	–12.40	130.90	–23.13	202.68	1.18	TERC, UNC	91/8–
Weipa	WEP	–12.68	141.88	–22.99	214.34	1.18	WNSS, UNC	90/7–
Birdsville	BSV	–25.54	139.21	–36.58	212.96	1.55	POB	90/7–
Dalby	DAL	–27.18	151.20	–37.09	226.80	1.57	DAC, UNC	91/8–
Canberra	CAN	–35.30	149.00	–45.98	226.14	2.07	IPS	94/8–
Adelaide	ADL	–34.67	138.65	–46.46	213.66	2.11	DSTO	90/7–
Kotzebue	KOT	66.88	197.40	64.52	249.72	5.40	UAF	93/11–
Ewa Beach	EWA	21.32	202.00	22.67	269.36	1.17	PTWC/USGS	91/1–
American Samoa	ASA	–14.28	170.70	–20.60	245.05	1.14		
Macquarie Isl.	MCQ	–54.50	158.95	–64.50	247.84	5.40	AAD	92/11–

*Includes established and proposed stations during the STEP period.

**The IGRF-90 model was used to calculate corrected geomagnetic coordinates and L values for 100-km altitude at each station on January 1, 1993.

***The Solar-Terrestrial Environment Laboratory, Nagoya University (STEL), is conducting multinationally coordinated magnetic observations in cooperation with and/or courtesy of the following institutes and organizations: University of Newcastle (UNC), Electronics Research Laboratory (DSTO), CSIRO Tropical Ecosystems Research Centre (TERC), Learmonth Solar Observatory and Canberra Observatory of IPS Radio and Space Services (IPS), Weipa North State School (WNSS), Birdsville Police Station (POB), Dalby Agriculture College (DAC), and Australian Antarctic Division (ADD) in Australia; National Institute of Aeronautics and Space (LAPAN), in Indonesia; Tohoku University (THU), Tohoku Institute of Technology (TIT), Kakioka Magnetic Observatory (KMO), Tokai University (TKU), University of Tokyo (GRL), and Kyushu University (UK) in Japan; Paradise Wewak Hotel (PWH) and University of Papua New Guinea (UPNG) in Papua New Guinea; Coast & Geodetic Survey Department (CGSD) in the Philippines; Institute of Space Research and Radiowaves (IKIR), Institute of Cosmo physical Research and Aeronomy (IKFIA), and Institute of Physics of Earth (IFZ) in Russia; Lunping Observatory (LNP), and National Central University (NCU) in Taiwan; and Guam Magnetic Observatory, U.S. Geological Survey (USGS), Pacific Tsunami Warning Center (PTWC), Koror Observatory of the U.S. National Weather Service and University of Alaska, Fairbanks (UAF) in the United States.

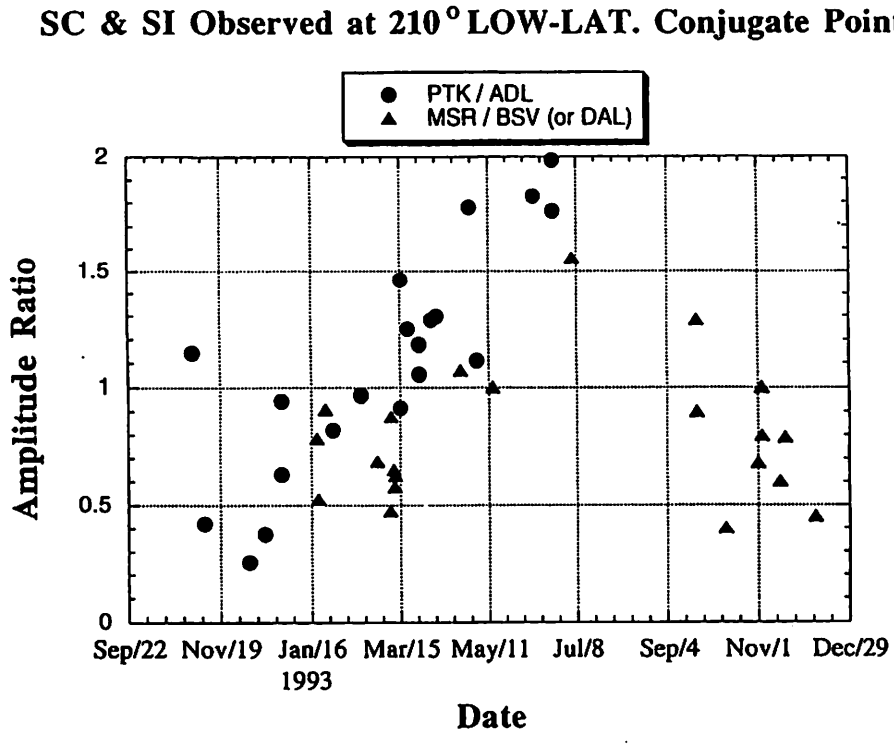

Fig. 2. Amplitude ratios of sc and si disturbances observed at low-latitude conjugate point pairs during the interval from November 1992 to December 1993. Solid circles and triangles indicate the ratio of sc and si amplitudes at Paratunka ($L = 2.10$) in the northern hemisphere to those at Adelaide (2.11) in the southern hemisphere and of those at Moshiri (1.59) to Birdsville (1.55) (or Dalby (1.57)), respectively.

We also used the 210° MM data to confirm the enhancement of sc and si amplitudes near the dayside equator.

Figure 2 shows the amplitude ratios of the sc and si disturbances observed at low-latitude conjugate point pairs during the interval from November 1992 to December 1993. Circles indicate the ratios of sc and si amplitudes at Paratunka ($L = 2.10$) in the northern hemisphere to those at Adelaide ($L = 2.11$) in the southern hemisphere, and triangles indicate the ratios of amplitudes at Moshiri (1.59) to those at Birdsville (1.55) (or Dalby (1.57)). A very clear seasonal variation in the ratio can be seen in Fig. 2. At low and middle latitudes, the amplitudes of sc and si in the summer hemisphere are about twice as great as those in the winter hemisphere.

The northern and southern hemisphere asymmetry of sc and si disturbances at middle and low latitudes cannot be explained by invoking the Chapman-Ferraro current on the magnetopause (cf. Matsuoka *et al.*, 1995). The asymmetry can be interpreted by invoking an asymmetry in the northern and southern hemisphere twin-vortex-type ionospheric currents, by invoking enhanced ionospheric conductivities in the summer hemisphere. The observations in Figs. 1 and 2 indicate that at low and middle latitudes, the DP component of sc and si is larger than the DL component; that electric field penetration into the equatorial ionosphere plays an important role in the transfer of energy from high latitudes to the magnetic equator.

2. Low-Latitude Aurorae

Recent optical and magnetic observations at Moshiri Observatory ($\theta = 44°22'$ N, $\phi = 142°16'$ E) of the Solar-Terrestrial Environment Laboratory (STEL), indicate that even during moderate magnetic storms, subvisual low-latitude aurorae sometimes appear in concert with $\Delta H > 50$ nT positive magnetic excursions and large-amplitude Pi magnetic pulsations around a minimum D_{st} index of ~–200 nT and/or

in concert with sudden decreases of D_{st} at a rate of >30 nT/h (Yumoto *et al.*, 1994a, b). Optical instrumentations (photometers, all-sky television cameras) were used to identify six occurrences of subvisual low-latitude aurorae at Moshiri and Rekubetsu ($\theta = 43.46°$N, $\phi = 143.77°$E, $L = 1.6$) in Hokkaido, Japan, during the period from February 1992 to September 1993 (Shiokawa *et al.*, 1994).

A geomagnetic storm began with an sc ($\Delta H \sim 133$ nT at Moshiri) at 1958 UT on May 9, 1992; developed rapidly from 0700 UT on the next day for the next 6 h; and reached a minimum D_{st} of –276 nT at 1300 UT during the middle hour of May 10, as shown in Fig. 3. Ordinary H-component magnetic variations during the main phase are presented as a function of station latitude along the 210° MM, that is, Moshiri, Kagoshima, Chichijima, and Guam in the northern hemisphere and Weipa, Birdsville, and Adelaide in the southern hemisphere. During the main phase of the storm on May 10, 1992, a positive magnetic bay and Pi 2 pulsation began at 1207 UT, and the all-sky television camera at Rekubetsu recorded a low-latitude aurora at 1209 UT (Shiokawa *et al.*, 1994a). The maximum ΔH perturbations during the main phase were 380 nT at Guam ($L = 1.01$) and 270 nT at Moshiri ($L = 1.59$), whereas the magnitudes of the positive ΔH excursions near 1200–1300 UT (shaded area, Fig. 3) were 110 nT at Moshiri and 55 nT at Guam.

Enlarged ordinary H- and D-component magnetograms from the southern hemisphere 210° MM

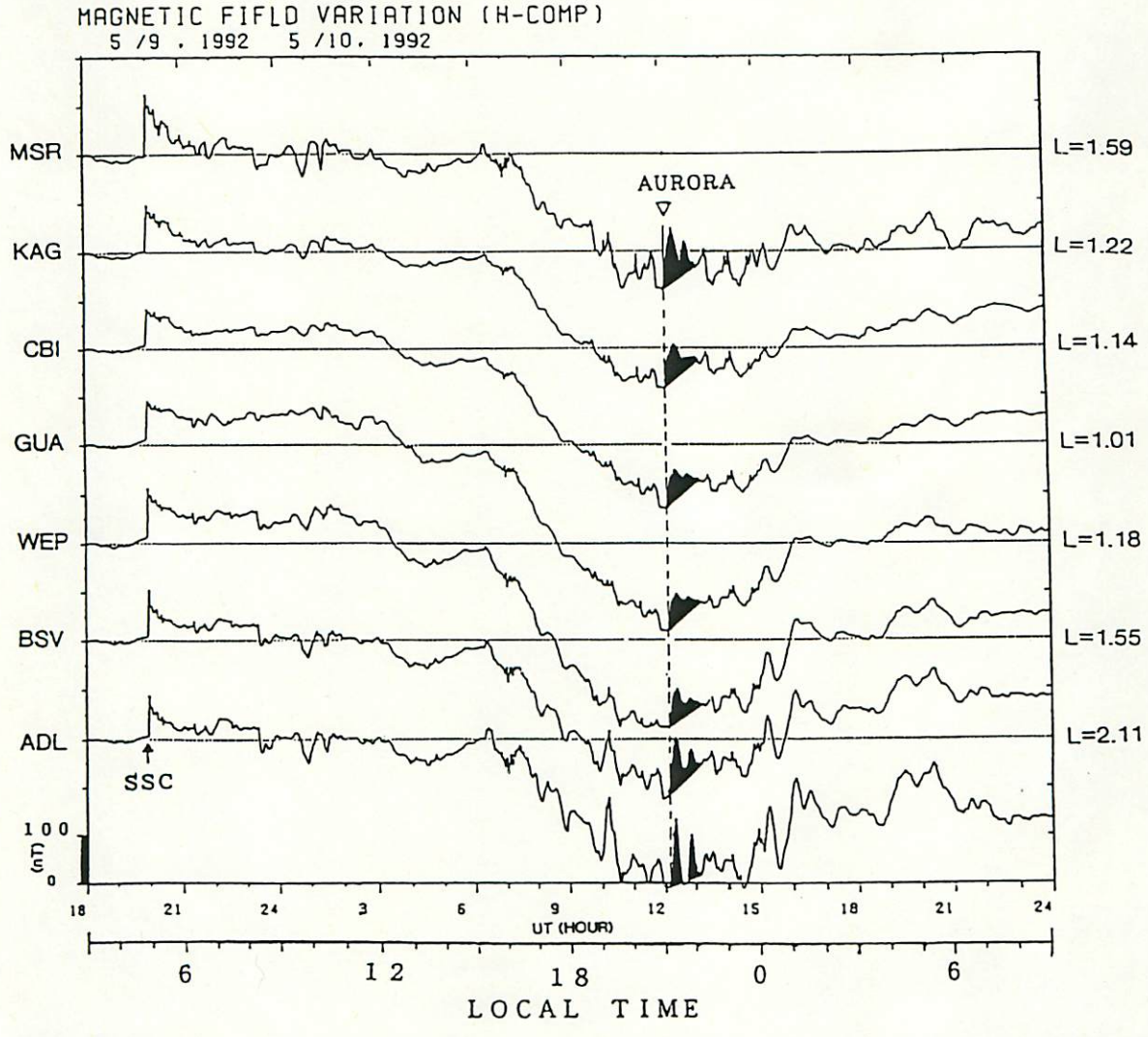

Fig. 3. Amplitude-time records of ordinary magnetic variations in ΔH during the main phase of the May 9–10, 1992, storm observed at 210° MM stations MSR, KAG, CBI, and GUA in the northern hemisphere and WEP, BSV, and ADL in the southern hemisphere. Solid areas indicate positive magnetic excursions associated with subvisual low-latitude aurora observed at Rekubetsu, Hokkaido, Japan.

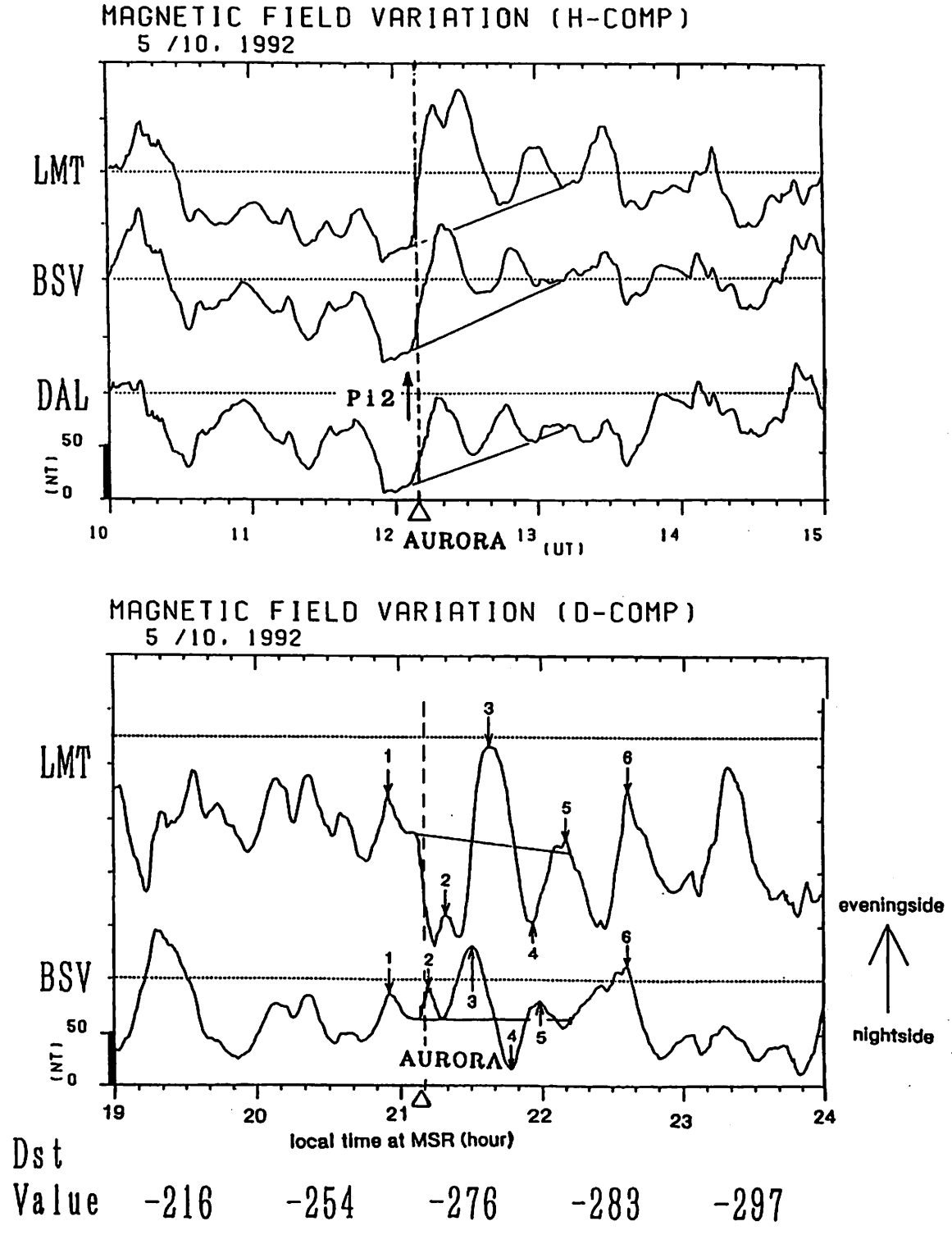

Fig. 4. Enlarged amplitude-time records of magnetic excursions in ΔH and ΔD observed at LMT, BSV, and DAL over 1000–1500 UT on May 10, 1992. Onset times of Pi 2 and auroral emission are indicated by an arrow and a broken line, respectively.

chain stations at Learmonth, Birdsville, and Dalby are given in Fig. 4 for the interval from 1000 to 1500 UT on May 10, 1992. Extremely large-amplitude Pi 2 magnetic pulsations were detected at 1207, 1443, and 1500 UT (not shown in the figure) by the 210° MM stations. The Learmonth, Birdsville, and Dalby stations are located at almost the same magnetic latitude and are listed in order of increasing magnetic longitude. Both the *H*- and *D*-component substorm variations at 1207 UT show apparent phase delays

from the midnight side toward the evening side during the premidnight sector. From the observed phase delays, the apparent longitudinal velocity (V_{app}) of the equivalent ionospheric current pattern near 40° magnetic latitude can be estimated as about 7 km/s westward. Figure 4 also shows interesting negative-positive magnetic deflections in the D component, that is, bipolar variations at Learmonth and Birdsville from 1207 to 1310 UT on May 10, 1992. The H-component variation during the low-latitude auroral event comprises two unipolar variations. The D-component variation resembles the negative time derivative of the H component. The bipolar structure of the D-component variations at L = 1.6–2.1 can be explained by the westward movement of an ionospheric Hall current vortex localized at middle latitudes around the low-latitude aurora (see Fig. 5 and/or Fig. 14 of Yumoto *et al.*, 1994b). The deflection of the D-component perturbations changes from westward to eastward at Learmonth and from eastward to westward at Birdsville, as shown in Fig. 4, suggesting the formation of an ionospheric Hall current vortex with an upward field-aligned current (FAC) near a meridian lying between Learmonth and Birdsville and the westward motion of this vortex through the premidnight sector at 1207 UT (=2107 JST) on May 10, 1992.

The equivalent ionospheric current vectors during the interval from 1207 to 1312 UT on May 10, 1992, shown in Fig. 5 were deduced by rotating the magnetic field vectors at Darwin, Weipa, Learmonth, Birdsville, Dalby, and Adelaide 90° clockwise. This procedure is appropriate when the dimensions of the ionospheric current system are much larger than the height of the ionospheric current layer. The current scale and station distribution are indicated in the bottom right and top left panels of Fig. 5, respectively. Open circles in the other panels represent observation sites. The magnetic variations at the ground stations are believed to result from a superposition of the substorm current wedge (McPherron *et al.*, 1973) and a local ionospheric current vortex around low-latitude aurorae. In order to distinguish the local variations associated with low-latitude aurorae from global variations caused by the substorm current wedge at higher latitudes, the perturbation field vectors at the six stations were redefined by deducting the magnetic field at Guam from the respective magnetic fields. Equivalent current vectors in Fig. 5 can be understood to relate mainly to low-latitude auroral variation. An equivalent current vortex with clockwise rotation which can be seen clearly between Learmonth and Adelaide after $t \sim 1212$ UT appears to move westward. Horizontal scales for the current vortex at 1227 UT are about $l_X \sim l_y \sim 3000$ km in the latitudinal and longitudinal directions. After 1245 UT, another current vortex appears east of Adelaide, moves westward, and disappears at around 1310 UT.

An FAC may flow upward near the center of the clockwise current vortex in the southern hemisphere. The magnitudes of the FACs can be estimated by assuming that the electric field associated with the low-latitude aurorae can be described as a quasi-static magnetic potential in the region below the ionosphere. The characteristic horizontal wave number is on the order of $k_\perp \sim 1.4 \times 2\pi/l_X \text{ km}^{-1}$. Ground magnetic field amplitudes (b_G) on the order of 75 nT for the 1227 UT event give $b_M \sim 52$ nT for the magnetic field above the ionosphere, assuming $b_G/b_M \sim (\Sigma_H/\Sigma_P)\exp(-110k_\perp)$ for a ratio of uniform ionospheric Hall and Pedersen conductivity (Σ_H/Σ_P) of 2 (Glassmeier, 1984). The upward FAC related to the low-latitude aurorae is on the order of $J_\parallel \sim b_M/(\mu_o l) \sim 1.4 \times 10^{-8}$ A/m^2. One can estimate the ionospheric electric field to be on the order of $\delta E_I = b_M/(\mu_o \Sigma_P) \sim 7$ mV/m for $\Sigma_P \sim 5$ S in the low-latitude auroral region.

All low-latitude aurorae observed in 1992 exhibit vortical equivalent ionospheric current patterns, and four of them also show westward movement (Yumoto *et al.*, 1994a). Although there is not yet sufficient evidence to provide this idea, we propose that the magnetic perturbations associated with the low-latitude aurorae correspond to changes in substorms and local overhead currents that involve strong perturbing forces on the trapped-particle population and precipitate large fluxes of low-energy electrons into the thermosphere. The large oscillations in the D component of the magnetic field can be explained by the intensification of an FAC(s) within ionospheric Hall current vortex (vortices) and their spatial movement, as shown in Fig. 15 of Yumoto *et al.* (1994b). The upward FAC must be associated with intense precipitation of energetic electrons at latitudes below that which is normal for the auroral oval. The direct injection of energy from the ring current in the form of particle precipitation into the upper thermosphere must be very significant and must affect the dynamics of the thermosphere and ionosphere during magnetically disturbed times. Particle precipitation into the low- and mid-latitude thermosphere and low-

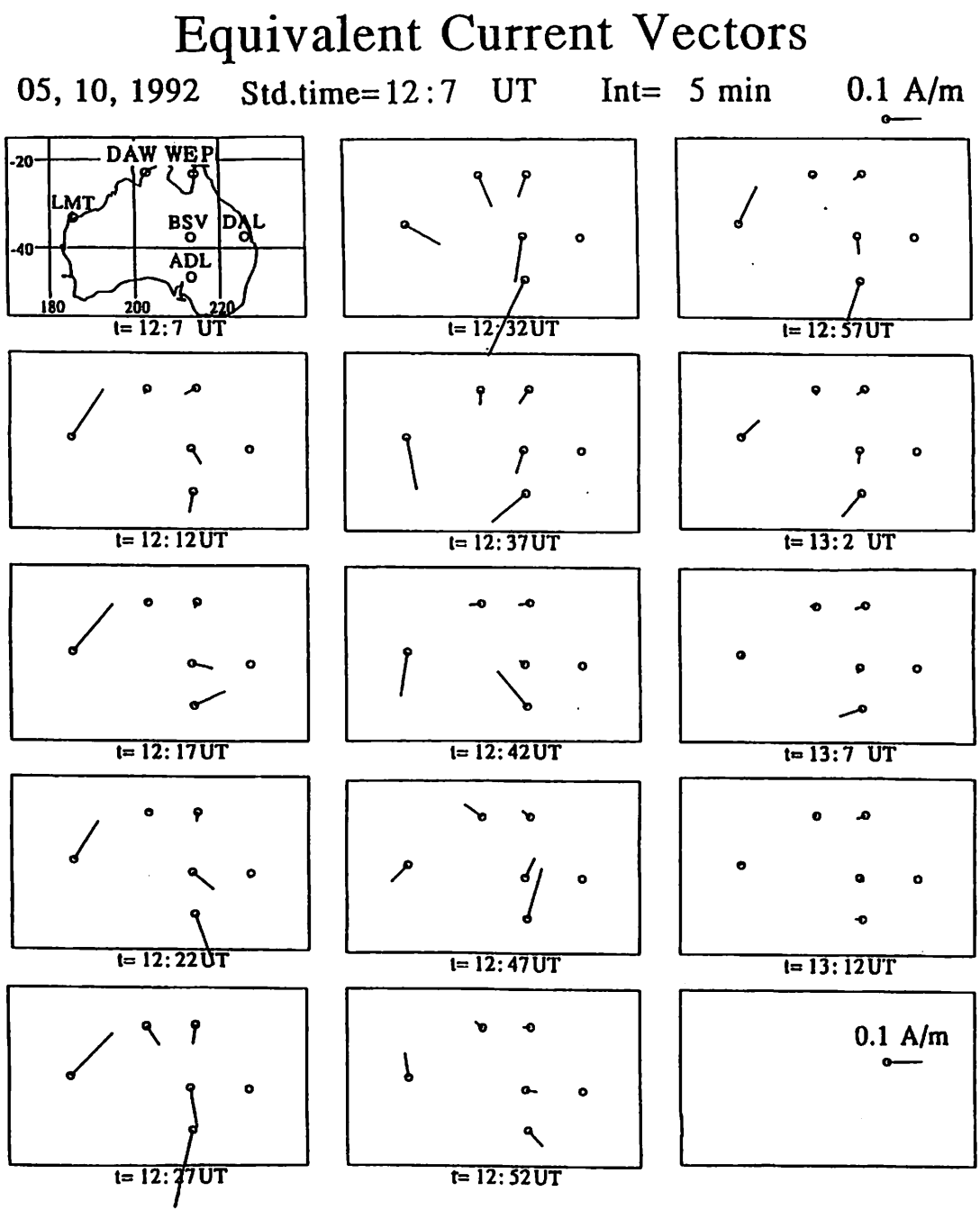

Fig. 5. Equivalent ionospheric current vectors deduced from magnetic variations at DAW, WEP, LMT, BSV, DAL, and ADL during the low-latitude auroral event of 1207–1312 UT on May 10, 1992. Equivalent ionospheric current vectors are obtained by rotating the magnetic perturbation vectors deducting the magnetic field at Guam from all the magnetic fields.

latitude aurorae coincides with large values of D_{st}, which are proportional to the total energy content of the trapped particles that constitute the ring current.

Shiokawa *et al.* (1995) recently used DMSP-F10 satellite plasma particle observations to confirm the intense precipitation of energetic electrons associated with the May 10, 1992, low-latitude aurora event. The electron precipitation did not appear in an expanded auroral oval but rather in an isolated region around 50° magnetic latitude. This precipitation exhibits an unusual acceleration process in which electrons at all energies measured (32 eV to 30 KeV) are intensified. Nevertheless, we conclude that the intensity variations of optical emissions and magnetic perturbations during low-latitude aurorae are

associated with variations in both the upward FAC (and/or electron precipitation) and the ring current strength in a localized region and on a shorter time scale. The low-latitude aurorae are evidence that solar wind energy can be transferred into the inner magnetosphere around $L = 2.5$ during magnetic storms.

3. Cavity-Like and Field-Line Pc 3-4 Oscillations Stimulated by si and sc

The 210° magnetometer network data were also analyzed to determine whether or not global cavity mode and localized field line oscillations can be excited in the inner magnetosphere by interplanetary impulses (sc and si) (Yumoto *et al.*, 1994c). It was found that two types of Pc 3-4 magnetic pulsations were stimulated at low latitudes just after 13 sc and si events. Most of the Pc 3-4 were standing field line oscillations, having maximum power densities at $L = 1.6$ and/or higher latitudes, while only four global cavity mode-like oscillations with larger amplitude at lower latitudes ($|\Phi| < 30°$) were stimulated by extremely large sc and si within the dayside plasmasphere.

In order to find low-latitude Pc 3-4 magnetic pulsations stimulated by magnetospheric impulses, we selected 13 sc and si events observed at six stations (MSR, CBI, KAG, WEP, BSV, ADL) along the 210° MM during local daytime, i.e., from 0500–1900 LT, during the period from July 21, 1990, to September 8, 1991. Power spectrum densities for 20-min intervals just before, just after, and 20 min after the sc and si onsets were calculated to identify spectral peaks at the separated low-latitude stations along the 210° MM and to clarify the latitudinal variation in the common spectral components in the Pc 3-4 frequency range. The power spectrum densities for the 20-min intervals were calculated by using the fast Fourier

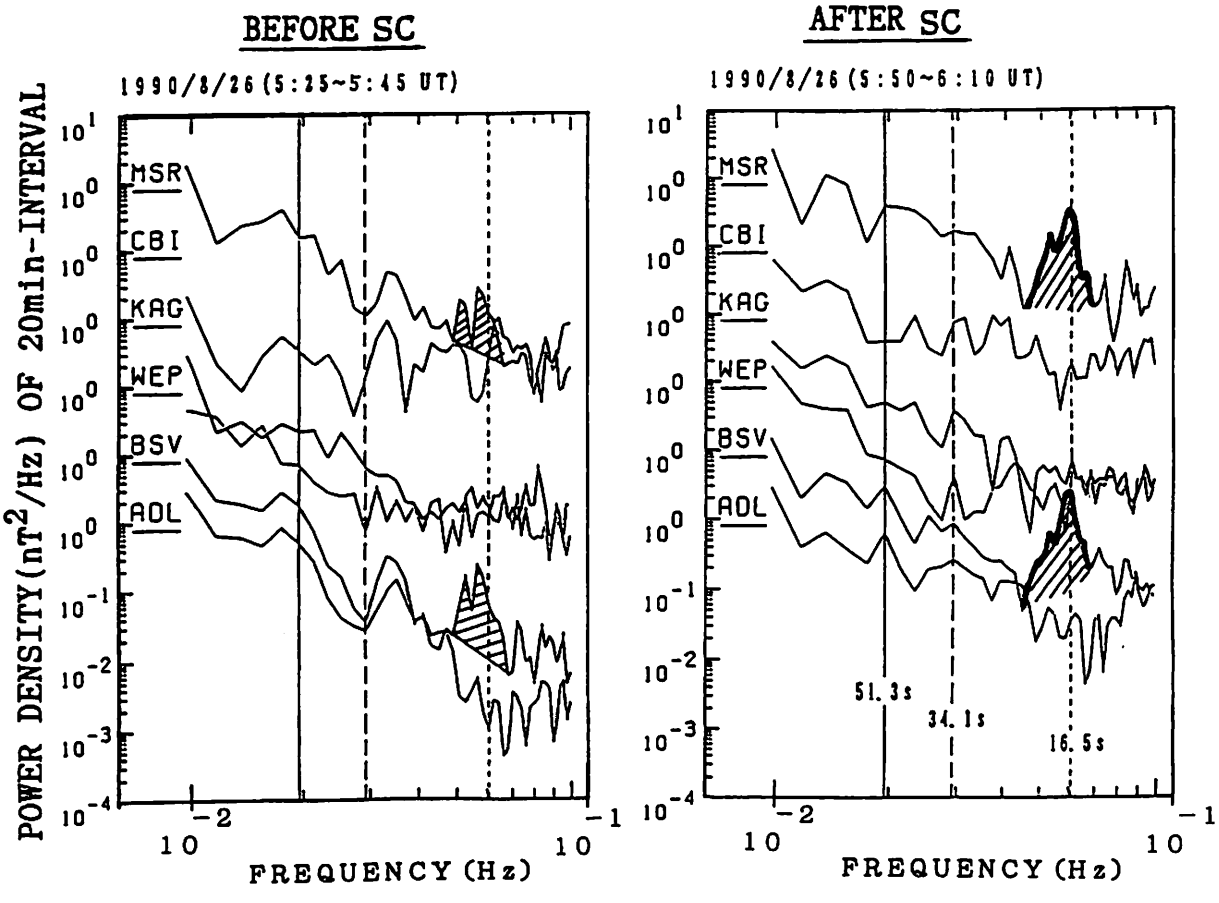

Fig. 6. Power spectrum curves of H-component magnetic data for each 20-min interval obtained from the 210° MM stations MSR, CBI, KAG, WEP, BSV, and ADL just before (left) and just after (right) the sc event with $\Delta H \sim 33$ nT at MSR at 0548 UT ($K_p = 3_+$) on August 26, 1990.

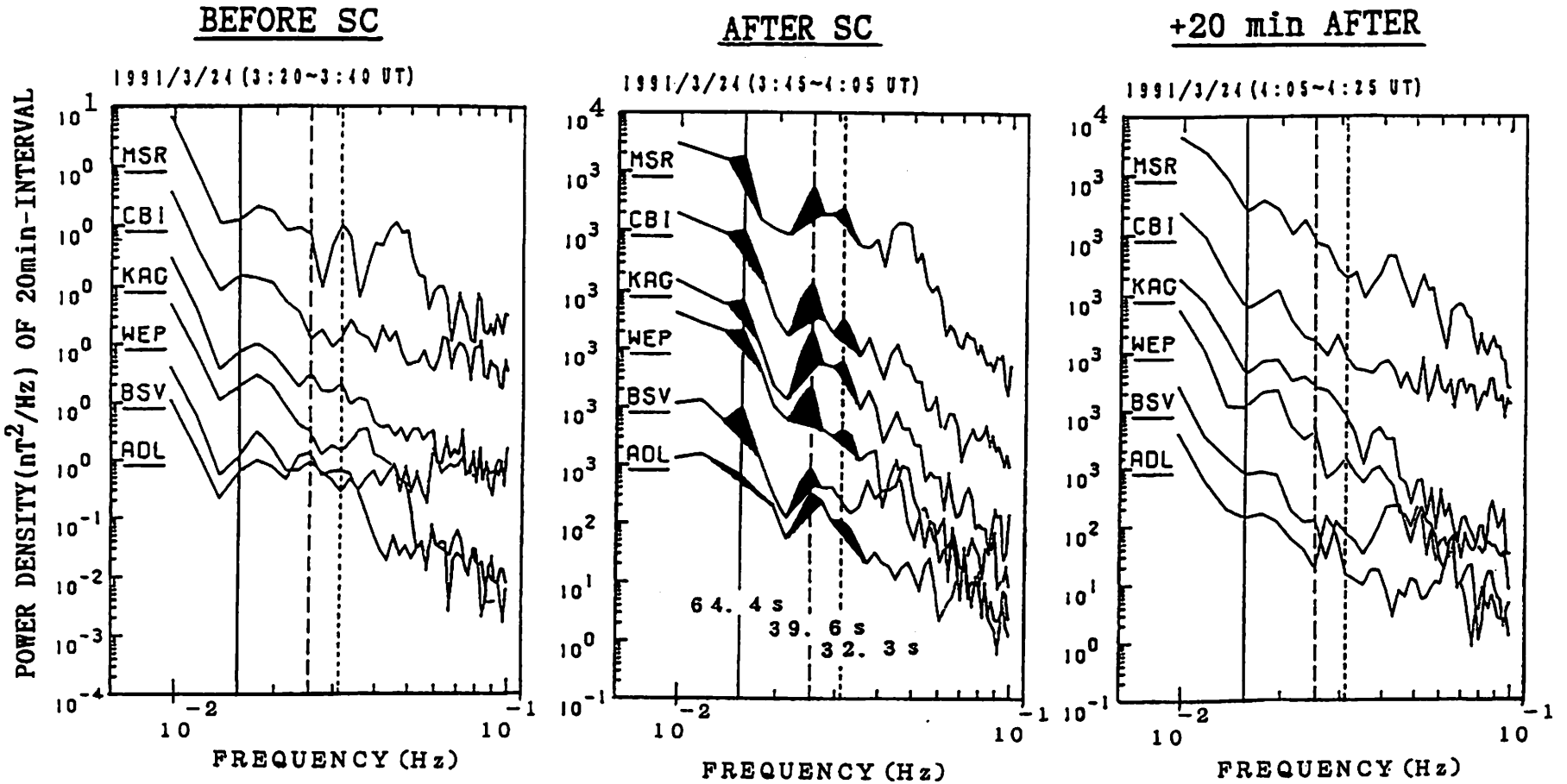

Fig. 7. Power spectrum curves of H-component magnetic data for each 20-min interval obtained from the MSR, CBI, KAG, WEP, BSV, and ADL stations just before (left), just after (middle), and 20 min after (right) the sc event with $\Delta H \sim 200$ nT at KAK at 0340 UT ($K_p = 9_-$) on March 24, 1991.

transform method. Then we examined wave characteristics to clarify which of the cavity mode-like and field line oscillations can be stimulated predominantly after the impulsive sc and si events in the real inner magnetosphere.

Figure 6 shows a typical example of power spectra for standing field line oscillations stimulated at low latitudes by a sudden impulse on August 26, 1990. The left and right panels indicate superimposed power spectrum curves of H-component magnetic variations observed at the six low-latitude stations during the intervals 0525–0545 UT just before and 0550–0610 UT just after the sc event, respectively. Power spectrum levels of pulsations after the sc event became slightly higher than those before the event. Three oscillations with identical discrete spectral components (T = 51.3, 34.1, and 16.5 s; vertical lines in the right panel) were excited just after the sc onset. It is noteworthy that the short-period components with 16- to 20-s periods are visible at low power levels in the spectra of MSR and BSV before the sc and were most effectively stimulated by the sc around the conjugate points of Moshiri and Birdsville (L = 1.55–1.59), identified by the shaded area in Fig. 6. This oscillation corresponds to the localized short-period (10–20 s) Pc 3 magnetic pulsation observed at low latitudes, i.e., a torsional Alfvén resonance oscillation around 38° magnetic latitude, as illustrated in Fig. 7 of Yumoto *et al.* (1992).

The other example of power spectrum densities of 20-min interval pulsation data at the six chain stations is shown in Fig. 7, which illustrates an example of cavity mode-like oscillations stimulated after an impulsive sc event. The left, middle, and right panels show superimposed power spectra of H-component magnetic variations observed during the intervals 0320–0340 UT just before the sc onset and 0345–0405 UT and 0405–0425 UT just after the event, respectively. Spectral levels of the pulsations after the sc event became $>10^3$ times higher than those before the event. Three identical spectral components (T = 64.4, 39.6, and 32.3 s period) were excited just after the onset of the sc event at different latitudes in the inner magnetosphere. The local standing field line oscillation with frequency near 45 mHz and maximum amplitude at MSR and BSV (L = 1.55–1.59) was also activated after the sc event. It is noteworthy that spectral peaks around T = 64.4 s (15.5 mHz), which did not exist before the sc but appeared after the event, show exactly the same frequency at the L = 1.1–2.1 meridional stations and similar power levels of $>10^3$ (nT^2/Hz). This component is indicated by a solid vertical line in the middle panel. Higher-frequency components at 39.6 s (25 mHz) and 32.3 s (31 mHz) were also stimulated after the sc onset. The right panel shows another interesting feature: these global Pc 3-4 pulsations with identical periods at

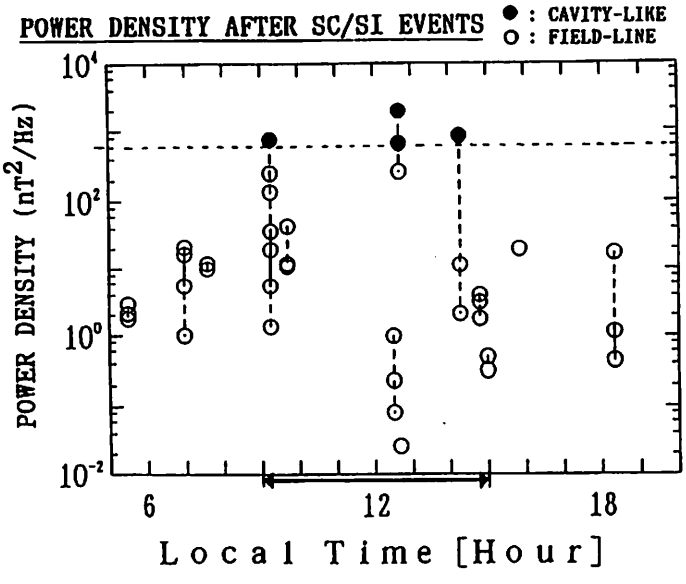

Fig. 8. Power densities of identical spectral peaks of Pc 3-4 magnetic pulsations stimulated just after the sc and si events as a function of local time at the 210° MM chain stations when the events happened. Solid and open circles indicate global cavity mode-like and localized standing field line oscillations, respectively.

different locations continued for about 20 min, and then disappeared concurrently. Identical periods at different latitudes and larger amplitudes at lower latitudes distinguish these pulsations from standing field line oscillations. They can be explained by invoking a cavity mode oscillation in the plasmasphere or magnetosphere (see references in Yumoto *et al.*, 1990; Lee and Lysak, 1990; Itonaga *et al.*, 1992; and Fujita and Glassmeier, 1993).

We also investigated the phase relationships of these stimulated oscillations. We used the latitudinal power density profile and phase relationships to classify the 38 identical stimulated spectral components listed in Table 2 of Yumoto *et al.* (1994c) into one of two magnetohydrodynamic modes of standing field line and cavity-like oscillations. Only four oscillations with longer periods, i.e., 64.4 and 39.6 s at 0340 UT on March 24, 85.0 s at 0517 UT on March 24, and 73. 5 s at 0015 UT on June 13, 1991, can be categorized as cavity mode-like oscillations, since they have a latitudinally broad, greater power density at lower latitudes. The remainder of the 34 oscillations were stimulated by the sc and si events as standing field line oscillations with a localized maximum power density at low latitudes. Figure 8 shows power spectrum peak densities of the 38 oscillations obtained at Moshiri just after the sc and si events as a function of magnetohydrodynamic mode and local time when the events happened. The solid and open circles indicate cavity mode-like and standing field line oscillations, respectively. Cavity mode-like oscillations tend to be observed only when the 210° MM chain stations are located within the daytime sector from 0900 to 1500 LT, the level of magnetic activity is $K_p > 7_+$, and the stimulated power density just after the sc event is larger than 600 nT^2/Hz (see Table 2 in Yumoto *et al.*, 1994c). This result implies that the interplanetary impulses must be sufficiently large to drive cavity mode-like waves. Pc 3-4 cavity mode-like oscillations at low latitudes are not easily stimulated by the external impulses in the solar wind and tend to be excited within the dayside plasmasphere only by great sc and si.

The observational results indicate that interplanetary impulses can readily stimulate Pc 3-4 standing field line oscillations but do not easily excite cavity-mode oscillations in the inner magnetosphere.

4. Peculiarities of Pc 3 pulsations at Low Latitudes

Magnetospheric ultra-low-frequency (ULF) field line oscillations at middle and high latitudes have been thoroughly studied for many years with the wide range of facilities of modern geophysics. However, much less is known about the physical nature of ULF waves at low latitudes and near-equatorial latitudes. Low-latitude magnetic field line oscillations may have a number of characteristic features that distinguish

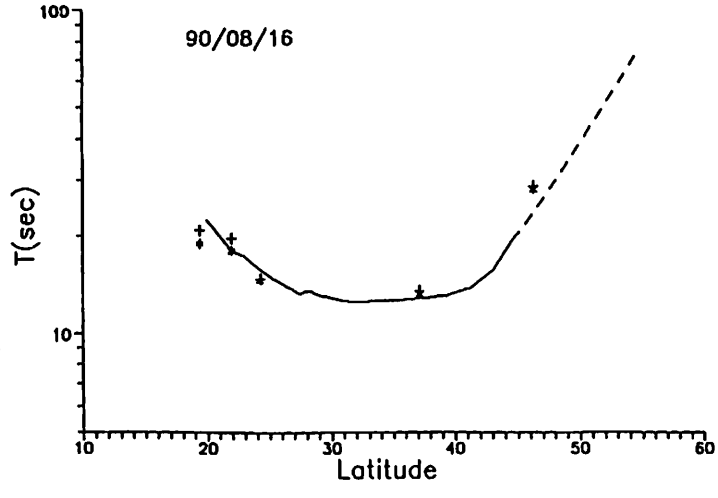

Fig. 9. Latitudinal profile of the field line resonance period for the IRI/AT model (solid line) corrected using the ground ionospheric observation data and for the empirical whistler/ISEE model (dashed line). The Pc 3 periods observed on August 16, 1990, along the low-latitude 210° MM chain stations are marked by asterisks and crosses.

them from the well-known mid-latitude geomagnetic pulsations (e.g., Yumoto *et al.*, 1995). These peculiarities are related to the essential influence of ionospheric ions on field line oscillations. New facilities for the experimental study of the spatio-spectral structure of ULF pulsations became available after the onset of the 210° MM project. Here, we demonstrate a peculiarity of Pc 3 pulsations at low latitudes, i.e., increasing period with decreasing magnetic latitude, and compare the observations with the results of numerical models of the magnetospheric resonator.

Figure 9 shows the latitudinal variation in the fundamental eigenperiod of the magnetospheric resonator and the observational result from the 210° MM data. Asterisks and crosses are dominant Pc 3 periods of the maximum entropy method (MEM) power spectra obtained at Adelaide ($L = 2.11$), Moshiri (1.59), Kagoshima (1.22), Weipa (1.18), and Chichijima (1.14) during the interval 0035–0100 UT on August 16, 1990. In order to estimate the eigenperiod of fundamental field line oscillations at low latitudes, we employed the empirical equatorial electron density model of Carpenter and Anderson (1992) based on whistler and the ISEE satellite data, and the field-aligned distribution of heavy ionospheric ions from the IRI/AT model (see Angerami and Thomas, 1964; Bilitza, 1992; Pilipenko *et al.*, 1995). The solid curve in Fig. 9 indicates the eigenperiod obtained numerically from the magnetospheric plasma model. At magnetic latitudes of >35°, we can see the standard increase in period with increasing magnetic latitude, whereas below a magnetic latitude of 30°, the abnormal reverse dependence is observed. The Pc 3 period increases monotonically toward the magnetic equator.

Magnetic data from the 210° MM network reveal a number of specific features of low-latitude Pc 3 pulsations, including an abnormal dependence of resonant period on L and a drastic increase in ionospheric damping (Yumoto *et al.*, 1995), i.e., a so-called mass loading effect on Pc 3-4 oscillations in the near-equatorial latitude ionosphere ($L < 1.5$). Although the predicted nonmonotonic dependence of the ULF eigenperiod on magnetic latitude has been experimentally supported, the observed periods are much shorter than those given by Poulter *et al.* (1990). Although a detailed comparison between the various ionospheric plasma models and observational data is required, ULF observations could be used as a low-latitude extension of whistler observations to monitor plasma density variations in the plasmasphere (Pilipenko *et al.*, 1995).

5. Latitudinal Profile of Pi 2

At the onset of magnetospheric substorms, transient hydromagnetic oscillations with periods of 40–150 s, called Pi 2 magnetic pulsations, are excited globally in the magnetosphere (Baumjohann and Glassmeier, 1984; Yumoto, 1986, 1988). One possible source of nighttime Pi 2 pulsations is a sudden change in magnetospheric convection or configuration during the substorm expansive phase (Akasofu, 1980), which would be caused by a plasma flow from the reconnection (or current disruption) region or by the formation of a substorm current wedge (McPherron *et al.*, 1973). Many workers have studied Pi 2 magnetic pulsations observed on the ground and in space; however, the generation and propagation mechanisms of these pulsations are still open to question.

Yumoto *et al.* (1989) proposed a possible scenario for the excitation and propagation mechanisms of substorm-associated global Pi 2 pulsations. At the onset of substorm expansion, hydromagnetic impulse disturbances are launched, perhaps in association with tail reconnection (or current disruption) in the near-Earth plasma sheet. Some of the disturbances can propagate along the field line in the Alfvén mode to the high-latitude ionosphere (e.g., Chang and Lanzerotti, 1975). On the other hand, compressional impulse signals with a broadband frequency spectrum can propagate across the ambient magnetic field into the dayside magnetosphere and excite a cavity resonance-like mode in the inner magnetosphere. The magnetospheric cavity mode wave further couples with a field line oscillation at lower latitudes.

In order to check the Yumoto *et al.* (1989) scenario, we analyzed data from stations along the 210° MM. Figure 10 shows one example of amplitude-time records of Pi 2 pulsations in the band-pass-filtered H-component (left) and D-component (right) magnetograms observed at the 210° MM chain stations at Tixie, Chokurdakh, Magadan, St. Paratunka, Moshiri, Kagoshima, Chichijima, and Guam in the northern

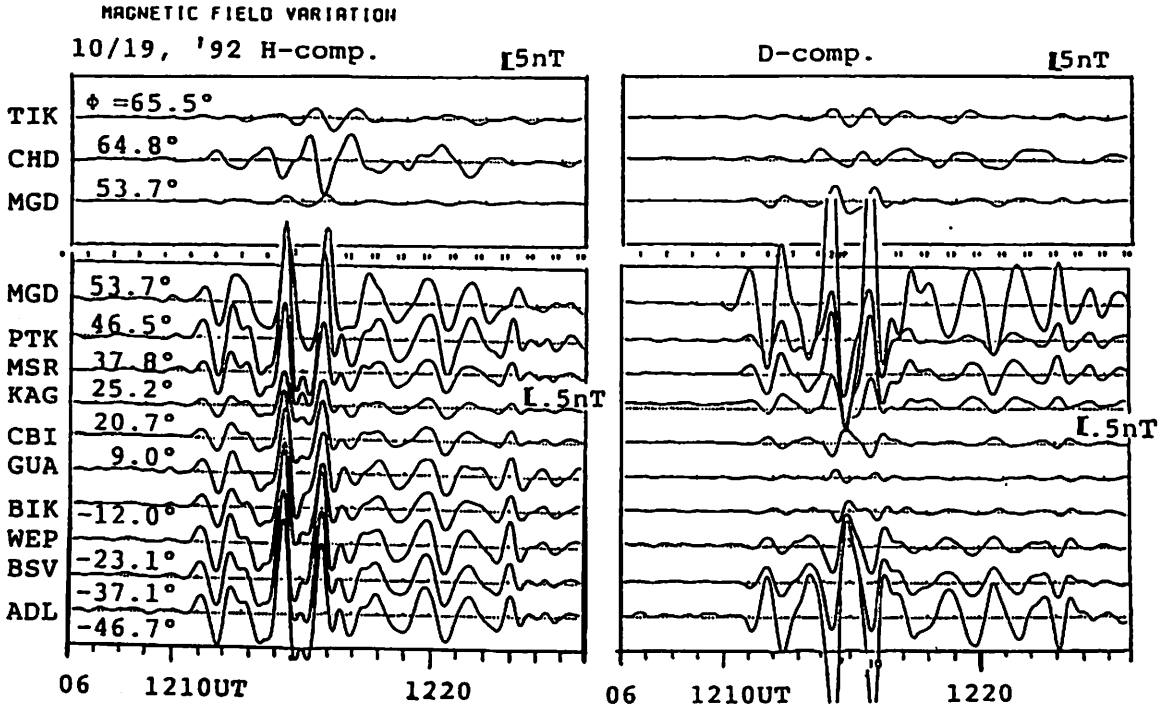

Fig. 10. Amplitude-time records of Pi 2 pulsations in ΔH and ΔD observed at the 210° MM stations TIK. CHD, MGD, PTK, MSR, KAG, CBI, and GUA in the northern hemisphere and BIK, WEP, BSV, and ADL in the southern hemisphere in the interval 1206–1226 UT on October 19, 1992. The frequency range of the bandpass filter is 6.7–26.7 mHz.

hemisphere and at Biak, Weipa, Birdsville, and Adelaide in the southern hemisphere from 1206 to 1226 UT on October 19, 1992. The frequency range of the band-pass filter is 6.7–26.7 mHz. We found the following for "low"-latitude Pi 2 pulsations: (1) Pi 2 pulsations have similar waveforms at lower latitudes; (2) *H*-component Pi 2 pulsations show an in-phase relation at the northern and southern stations, and *D* components show a 180° out-of-phase relation between the northern and southern stations; and (3) amplitudes of the *H* components are independent of geomagnetic latitudes and are almost the same at all stations, but *D* components depend on latitude and increase exponentially from the magnetic equator to higher latitudes, as shown in Fig. 11. Observational facts 1 and 2 suggest that the field line resonance theory (e.g., Hasegawa and Chen, 1974; Southwood, 1974) is inadequate to explain all of the characteristics of low-latitude Pi 2 pulsations. The eigenperiod of the field line oscillations varies from one field line to another; it depends on the length of the field line, the field strength, and the plasma density along the field line concerned. If each field line oscillates with its own eigenperiod, the dominant period of magnetic pulsations should vary from place to place (Nishida, 1978). Existing Pi 2 models of global cavity mode (e.g., Kivelson and Southwood, 1986; Allan *et al.*; 1986) and substorm current wedge (e.g., Lester *et al.*, 1983) can explain the nature of simultaneous occurrence and similarity of the waveform at low latitudes.

Figure 11 shows the averaged amplitude ratios normalized to Moshiri for the *H* and *D* components of Pi 2 pulsations observed at northern stations (Guam, Chichijima, Kagoshima, Moshiri, Magadan, Zyryanka (L = 3.91), Chokurdakh) in the 210° MM chain. It is noteworthy that the *H*-component amplitudes of Pi 2 pulsations are almost the same from Guam to Magadan and that those at Chokurdakh are roughly 1 order of magnitude larger. On the other hand, the *D*-component amplitudes of Pi 2 pulsations increase exponentially from Guam to Magadan and abruptly increase from near (or outside) the plasmapause, Zyryanka to Chokurdakh.

Figure 12 shows the phase relation of Pi 2 pulsations observed at Magadan, Zyryanka, and Chokurdakh to those at Moshiri for the *H* and *D* components. *H*-component Pi 2 pulsations at Moshiri and Magadan show an in-phase relation, while those at Moshiri and Chokurdakh show a 180° out-of-phase

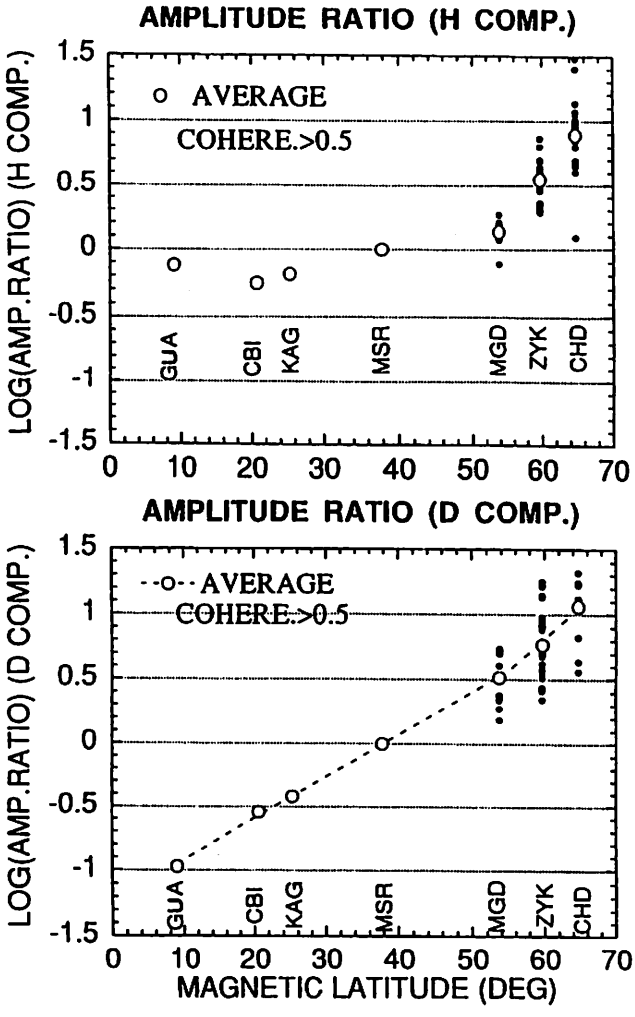

Fig. 11.

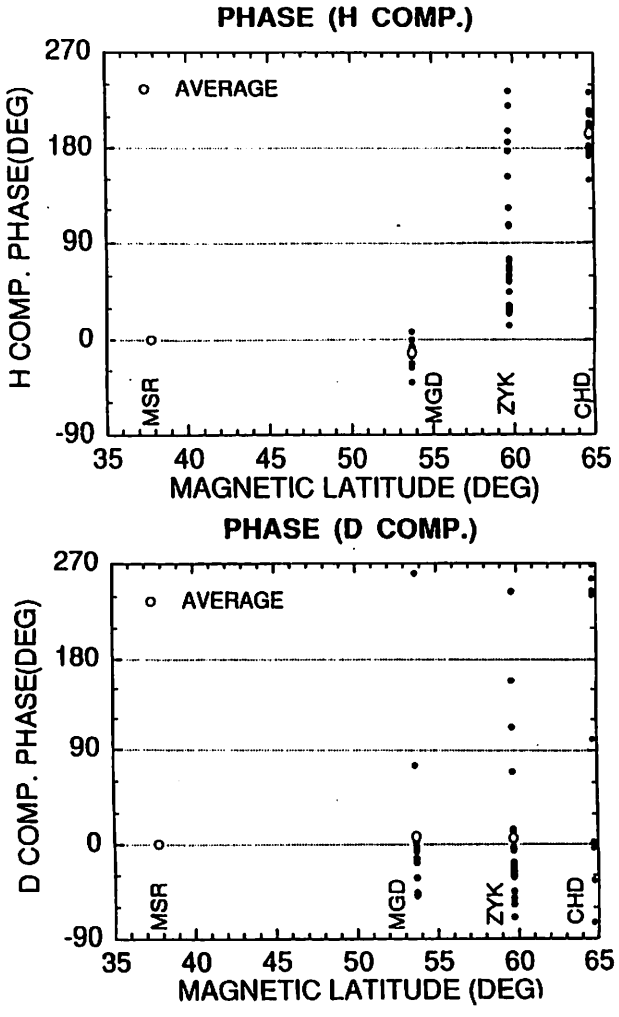

Fig. 12.

Fig. 11. Amplitude ratios of Pi 2 pulsations observed at northern stations (GUA, CBI, KAG, MSR, MAG, ZYK and CHD) of the 210° MM chain to those at Moshiri. The average values at GUA, CBI, KAG, and MSR were obtained by Yumoto *et al.* (1994d). (Top) *H* components; (bottom) *D* components.

Fig. 12. Phase relations of Pi 2 pulsations observed at MAG, ZYK, and CHD to those observed at MSR. (Top) *H* components; (bottom) *D* components.

relation. At Zyryanka near the plasmapause, *H*-component Pi 2 pulsations show a transitional phase relation from 0° to 180° to those at Moshiri. *D*-component Pi 2 pulsations at Moshiri, Magadan, and Zyryanka show an almost in-phase relation, but the phase relation of *D* components at Moshiri and Chokurdakh cannot be concluded. Half of the *D*-component Pi 2 events at Chokurdakh and Moshiri showed a poor coherence of less than 0.5 and were omitted in Figs. 11 and 12. The data from Moshiri and Chokurdakh in Fig. 12 showed too large a spread for any conclusions to be drawn.

From the observed latitudinal characteristics, Pi 2 magnetic pulsations may be explained by a global cavity mode oscillation with phase reversal near the plasmapause, the substorm current wedge model-like oscillation, and auroral field line oscillations with field-aligned and ionospheric current variations. However, it is still an open question whether the Yumoto *et al.* (1989) scenario is consistent with these observational results. In order to answer the question, in the near future we will further analyze the 210° MM chain data, including data from around the plasmapause and simultaneously obtained by the ISTP (AKEBONO, GEOTAIL) satellites.

6. Summary and Conclusion

From analyses of coordinated ground-based data along the 210° MM chain stations, the following initial results were obtained;

(1) Northern and southern hemisphere asymmetry of sc and si disturbances at low and middle latitudes indicates that the DP component of sc and si is larger than the DL component; i.e., electric field penetration into the equatorial ionosphere plays an important role in the transfer of energy from high latitudes to the magnetic equator.

(2) The low-latitude aurorae provide evidence that solar wind energy can be transferred into the inner magnetosphere around $L = 2.5$ during magnetic storms.

(3) The interplanetary impulses can readily stimulate a standing Pc 3-4 field line oscillation in the inner magnetosphere but don't easily excite cavity resonance oscillations at low latitudes. Only great sc and si can stimulate cavity-like oscillations within the daytime plasmasphere.

(4) Pc 3 at low latitudes indicates an abnormal dependence of the resonant period on L and a drastic increase in ionospheric damping, i.e., a so-called mass loading effect on Pc 3 oscillations in the near-equatorial latitude ionosphere ($|\Phi| < 30°$).

(5) The latitudinal profiles of Pi 2 phase relations and amplitudes imply that Pi 2 pulsations observed at low and high latitudes consist of different mode oscillations.

Imaging the Earth's magnetosphere using ground-based magnetometer arrays can be reconfirmed as one of the major techniques for investigating the dynamism of solar wind-magnetosphere interactions. Magnetic field l-s data from coordinated ground stations make it possible to study magnetospheric processes by separating the temporal changes and spatial variations of the phenomena, to clarify global and latitudinal structures and propagation characteristics of magnetic variations from higher to equatorial latitudes, and to understand the global generation mechanisms of the magnetospheric phenomena.

The author expresses his sincere thanks to all members of the 210° MM Magnetic Observation Project for their ceaseless support. The magnetic observations are being carried out by the STEL in cooperation with 27 institutes in Australia, Indonesia, Japan, Papua New Guinea, Philippines, Russia, Taiwan and the United States. We are grateful to D. G. Sibeck for his useful comments and suggestions. Thanks are due the Ministry of Education, Science, and Culture of Japan for financial support in the form of Grants-in-Aid for Overseas Scientific Survey (02041039, 04044077, 05041060, 06044094), Developmental Scientific Research (02504002), and the International STEP project.

REFERENCES

Akasofu, S.-I., What is a magnetospheric substorm?, in *Dynamics of the Magnetosphere*, edited by S.-I. Akasofu, pp. 447–460, D. Reidel, Norwell, Mass., 1980.

Allan, W., E. M., Poulter, and S. P. White, Hydromagnetic wave coupling in the magnetosphere-plasmapause effects on impulse excited resonances, *Planet. Space Sci.*, **34**, 1189–2000, 1986.

Angerami, J. J. and J. O. Thomas, Studies of planetary atmospheres, *J. Geophys. Res.*, **69**, 4537–4542, 1964.

Araki, T., A physical model of the geomagnetic sudden commencement, *AGU Geophysical Monograph*, **81**, 183–200, 1994.

Baumjohann, W. and K.-H. Glassmeier, The transient response mechanism and Pi 2 pulsations at substorm onset-Review and outlook, *Planet. Space Sci.*, **32**, 1361–1370, 1984.

Bilitza, D., Solar-terrestrial models an(l application software, *Planet. Space Sci.*, **40**, 541–579, 1992.

Carpenter, D. L. and R. R. Anderson, An ISEE/whistler model of equatorial electron density in the magnetosphere, *J. Geophys. Res.*, **97**, 1097–1108, 1992.

Chang, R. P. and L. J. Lanzerotti, On the generation of magnetohydrodynamic waves at the onset of substorm, *Geophys. Res. Lett.*, **2**, 489–491, 1975.

Fujita, S. and K.-H. Glassmeier, Cavity-mode magnetohydrodynamic oscillations with energy leakage through the outermost L-shell, *J. Geomag. Geoelectr.*, 1993 (to be submitted).

Glassmeier, K.-H., On the influence of ionospheres with non-uniform conductivity distribution on hydromagnetic waves, *J. Geophys. Res.*, **54**, 125–137, 1984.

Hasegawa, A. and L. Chen, Theory of magnetic pulsations, *Space Sci. Rev.*, **16**, 347–359, 1974.

Itonaga M., T.-I. Kitamura, O. Saka, H. Tachihara, M. Shinohara, and A. Yoshikawa, Discrete spectral structure of low-latitude and equatorial Pi 2 pulsation, *J. Geomag. Geoelectr.*, **44**, 253–259, 1992.

Kivelson, M. G. and D. J. Southwood, Coupling of global magnetospheric MHD eigen-modes to field line resonances, *J. Geophys. Res.*, **91**, 4345–4351, 1986.

Lee, D.-H. and R. L. Lysak, Effects of azimuthal asymmetry on ULF waves in the dipole magnetosphere, *Geophys. Res. Lett.*, **17**, 53–56, 1990.

Lester, M. W., J. Hughes, and H. J. Singer, Polarization pattern of Pi 2 magnetic pulsations and the substorm current wedge, *J. Geophys. Res.*, **88**, 7958–7966, 1983.

Matsuoka, H., K. Takahashi, K. Yumoto, B. J. Anderson, and D. G. Sibeck, Observation and modeling of compressional Pi 3 magnetic pulsations, *J. Geophys. Res.*, **100**, 12103–12112, 1995.

McPherron, R. L., C. T. Russell, and M. P. Aubry, Satellite studies of magnetospheric substorms on August 15, 1968, 9, Phenomenological model for substorm, *J. Geophys. Res.*, **78**, 3131–3149, 1973.

Nishida, A., *Geomagnetic Diagnosis of the Magnetosphere*, Springer-Verlag, Berlin, 1978.

Pilipenko, V. A., K. Yumoto, E. Fedorov, N. Kurneva, and F. Menk, Some peculiarities of field line Alfvén oscillations at low latitudes, *J. Geophys. Res.*, 1995 (to be submitted).

Poulter, E. M., W. Allan, and G. J. Bailey, The effect of density inhomogeneity on standing Alfvén wave structure, *Planet. Space Sci.*, **38**, 665–673, 1990.

Shiokawa, K., K. Yumoto, T. Oguti, Y. Tanaka, and Y. Kiyama, Low-latitude aurorae observed at Moshiri and Rikubetsu (L = 1.6) during magnetic storms, *J. Geomag. Geoelectr.*, **46**, 231–252, 1994.

Shiokawa, K., K. Yumoto, N. Nishitani, P. T. Newell, and C.-I. Meng, The substorm-associated low-latitude aurora excited by intense precipitation of energetic electrons during magnetic storms, *Nature*, 1995 (to be submitted).

Southwood, D. J., Some features of field line resonances in the magnetosphere, *Planet. Space Sci.*, **22**, 483–491, 1974.

Yumoto, K., Generation and propagation mechanisms of low-latitude magnetic pulsations—A review, *J. Geophys.*, **60**, 79–105, 1986.

Yumoto, K., External and internal sources of low-frequency MHD waves in the magnetosphere—A review, *J. Geomag. Geoelectr.*, **40**, 293–311, 1988.

Yumoto, K., K. Takahashi, T. Sakurai, P. R. Sutcliffe, S. Kokubun, H. Luhr, T. Saito, M. Kuwashima, and N. Sato, Multiple ground-based and satellite observations of global Pi 2 magnetic pulsations, *J. Geophys. Res.*, **94**, 3611–3618, 1989.

Yumoto, K., S. Watanabe, and H. Oya, MHD responses of a model magnetosphere to magnetopause perturbations, *Proc. Res. Inst. Atmos., Nagoya Univ.*, **37**, 17–36, 1990.

Yumoto, K., Y. Tanaka, T. Oguti, K. Shiokawa, Y. Yoshimura, A. Isono, B. J. Fraser, F. W. Menk, J. W. Lynn, M. Seto, and 210° MM Magnetic Observation Group, *J. Geomag. Geoelectr.*, **44**, 261–276, 1992.

Yumoto, K., T. Endo, K. Shiokawa, Y. Tanaka, and 210° MM Magnetic Observation Group, Ionospheric current and magnetic variations caused by low-latitude aurorae, in *COSPAR Colloquia Ser. Vol. 7 on Low-Latitude Ionospheric Physics*, pp. 241–250, edited by Fu-Shong Kuo, Pergamon Press, 1994a.

Yumoto, K., K. Shiokawa, T. Endo, Y. Tanaka, T. Oguti, and F. W. Menk, Characteristics of magnetic variations caused by low-latitude aurorae observed around 210° magnetic meridian, *J. Geomag. Geoelectr.*, **46**, 213–229, 1994b.

Yumoto, K., A. Isono, K. Shiokawa, H. Matsuoka, Y. Tanaka, F. W. Menk, B. J. Fraser, and 210° MM Magnetic Observation Group, Global cavity mode-like and localized field-line Pc 3-4 oscillations stimulated by interplanetary impulse (si/sc): Initial results from the 210° MM magnetic observations, *AGU Geophysical Monograph*, **81**, 335–344, 1994c.

Yumoto, K., H. Osaki, K. Fukao, K. Shiokawa, Y. Tanaka, S. I. Solovyev, G. Krymskij, E. F. Vershinin, V. F. Oshinin, and 210° MM Magnetic Observation Group, Correlation of high- and low-latitude Pi 2 magnetic pulsations observed at 210° magnetic meridian chain stations, *J. Geomag. Geoelectr.*, **46**, 925–935, 1994d.

Yumoto, K., V. A. Pilipenko, E. Fedorov, N. Kurneva, and K. Shiokawa, The mechanisms of damping of geomagnetic pulsations, *J. Geomag. Geoelectr.*, **47**, 163–176, 1995.